DOI: 10.1002/anie.200604261

Coronenes

Designing Paramagnetic Circulenes[**]

*Guglielmo Monaco, Patrick W. Fowler, Mark Lillington, and Riccardo Zanasi**

In an axial magnetic field, the annular molecules coronene, corannulene, kekulene, and nonplanar [7]circulene support disjoint, counterrotating, diatropic-rim/paratropic-hub ring currents.[1] This remarkable feature represents a failure of the very popular "annulene within an annulene" (AWA) model.[2] On the other hand, a circulene comprising 10 fused pentagons around a central decagon, namely [10,5]coronene (**1**), is predicted to have inverted counterrotating paratropic-rim/diatropic-hub ring currents.[3] In this case, the outer and inner cycles, which contain respectively 20 ($4n$) and 10 ($4n+2$) carbon atoms, are essentially decoupled and here the AWA picture *is* compatible with the ab initio result. For all these systems, the ipsocentric approach[4] provides a unified account of the opposed currents in terms of simultaneous translational and rotational π–π^* virtual excitations, and so provides a basis for further prediction and possible control of magnetic response properties in potential materials applications. For example, extensive paratropic (antiaromatic) perimeter circulation is an unusual property that is reflected in calculated magnetizability and nuclear magnetic shieldings, even when partially cancelled by the effects of a central diatropic current, as in **1**.[3] Can we eliminate the cancellation and achieve greater paratropicity by reversing the central current? Here we predict that two closed-shell neutral circulenes, **2** and **3**, support disjoint conrotating paratropic ring currents on both rim and hub. Indeed, the calculations indicate that **2** and **3** have a net paramagnetic response in one direction, and that in **3**, remarkably, this outweighs the diamagnetic contributions to magnetizability to give a closed-shell paramagnetic molecule. Retention of paratropic current at equilibrium geometry is rare, and the received wisdom is that antiaromatic molecules will exhibit fluxionality[5] or distort to "escape" their antiaromaticity.[6]

The aim is to find π systems based on a circulene-like template, but with conrotating paratropic currents on both outer and inner cycles of carbon atoms. For annular belts of hexagonal rings, it has been shown[1,7] that coupling of inner and outer circuits leads to counterrotation of ring currents. A belt of $2m$ fused pentagons around a central $2m$-gon, as in the case of **1**, has four Kekulé structures corresponding to the pairings of the two conjugated structures on rim and hub cycles. In all four, the radial 5/5 graph edges are formal single bonds and hence have zero Pauling π bond order. Thus, inner and outer circuits are decoupled, and this suggests that the AWA picture is applicable to this electronic structure. When $2m=4n$, the inner cycle should be antiaromatic; the outer $4m$ cycle should always be antiaromatic, independent of m. Two series of molecules can be postulated: one with $2m=4n+2$, for which the AWA picture predicts counterrotating (paratropic-rim/diatropic-hub) ring currents, as in the case of **1**, and a second with $2m=4n$, for which AWA would predict the desired pattern of conrotating paratropic ring currents. Realistic candidates can be obtained from **1** by changing the number of pentagons by two at a time. The new systems are [8,5]coronene (**2**) and [12,5]coronene (**3**; see Scheme 1), which are both expected to be nonplanar.

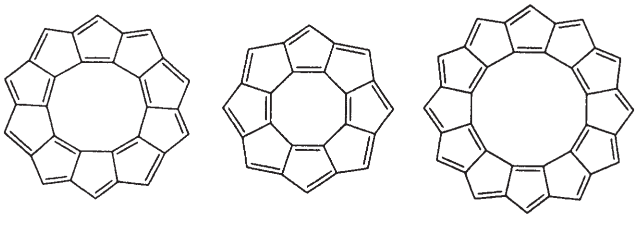

1 2 3

Scheme 1. Planar (C_{10h}) [10,5]coronene (**1**), bowl-shaped (C_4) [8,5]coronene (**2**), and quasi-saddle-shaped (C_2) [12,5]coronene **3**.

Optimized structures for **2** and **3** were by using Gaussian 03[8] at the B3LYP/6-31G* level, initially with maximum symmetry, to yield structures with imaginary frequencies that on relaxation along the imaginary-frequency modes reached local minima of C_4 and C_2 symmetry, respectively. The optimal structures were used in the further calculations of first-order current-density maps and magnetic properties. Bond lengths in **2** (see the Supporting Information) indicate a degree of bond fixation on both inner 8π and outer 16π cycles, and single bonds on radial edges. Bond lengths in **3** correspond to a degree of bond fixation within the 12π inner cycle, single bonds on the radial edges of the graph, and partial double bonds around the 24π outer cycle.

In both molecules σ/π mixing is substantial, but descendants of the p orbitals can be identified. In **2**(C_4) the 12 doubly occupied π orbitals of [8,5]coronene span the representation $3A+3B+3E$ (HOMO, HOMO-1, and HOMO-2 of B, A, and E symmetry, respectively.) In **3**(C_2) the 18 doubly

---

[*] Dr. G. Monaco, Prof. R. Zanasi
Department of Chemistry
University of Salerno
via Ponte don Melillo, 84084 Fisciano (SA) (Italy)
Fax: (+39) 089-969-603
E-mail: rzanasi@unisa.it
Prof. P. W. Fowler, M. Lillington
Department of Chemistry
University of Sheffield
Sheffield S3 7HF (UK)

[**] Financial support from University of Salerno, the Italian Ministero dell'Istruzione, dell'Università e della Ricerca (MIUR) the Royal Society/Wolfson Research Merit Scheme, and EPSRC is gratefully acknowledged.

Supporting information for this article is available on the WWW under http://www.angewandte.org or from the author.

occupied π orbitals of [12,5]coronene span 9A + 9B. (HOMO, HOMO−1, and HOMO−2, of which the last-named is a near-degenerate pair, are of A, B, and B symmetry, respectively.)

Current density maps were calculated with the CTOCD method[9] according to the ipsocentric approach at the 6-31G**//B3LYP/6-31G* level by using SYSMO.[10] Figures 1 and 2 display the total current arising from the set of 12 and 18 π orbitals of **2** and **3**, respectively, and the separate contributions to these totals from HOMO, HOMO−1, and HOMO−2 pair. Each map shows the calculated current density per unit field, induced by an external magnetic field oriented along the main symmetry axis of the molecule, and plotted on a surface having the molecular shape at a distance of $1a_0$ from the molecule. In the case of **2** the plotting surface is inside the bowl; on the outside (see Figure S1 in the Supporting Information) current circulates in much the same way but is weaker, as is expected from the poorer p-orbital overlap. The current pattern is indeed characterized by conrotating paratropic currents on inner and outer cycles, and the two circulations arise mainly from the nondegenerate HOMO and HOMO−1. The HOMO provides the inner circulation in **2** and the outer circulation in **3**, and vice versa for HOMO−1. The circulation arising from the HOMO−2 pair is diatropic on the outer cycle in both molecules, but weak. In contrast to **1**,[3] both **2** and **3** have a paratropic inner current that cooperates with the outer current to provide the

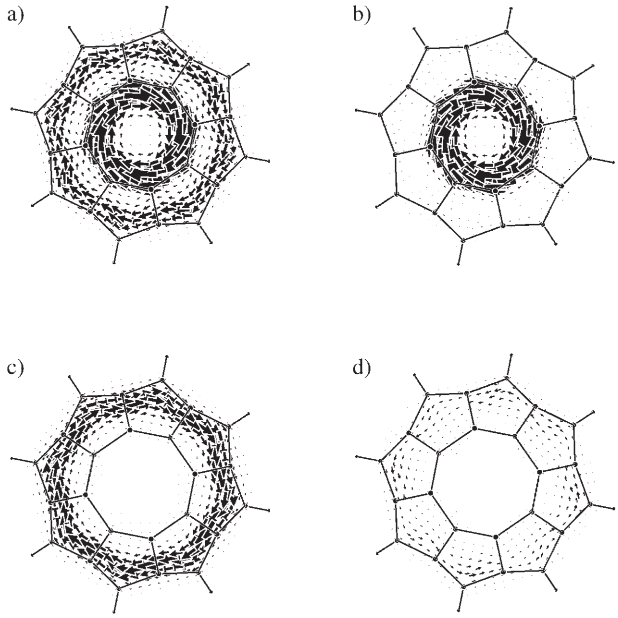

Figure 1. Maps of current density induced in the π system of [8,5]coronene by a perpendicular external magnetic field. The current density was calculated at the ab initio CTOCD-DZ2/6-31G**//B3LYP/6-31G* level and plotted on a surface with the molecular shape at $1a_0$ inside the bowl. a) Total current density arising from the set of 12 π orbitals and contributions of b) B π HOMO, c) A π HOMO−1, and d) E π HOMO−2 pair. Arrows indicate the direction and relative magnitude of the current density vector. Paratropic/diatropic currents are represented by clockwise/anticlockwise circulations.

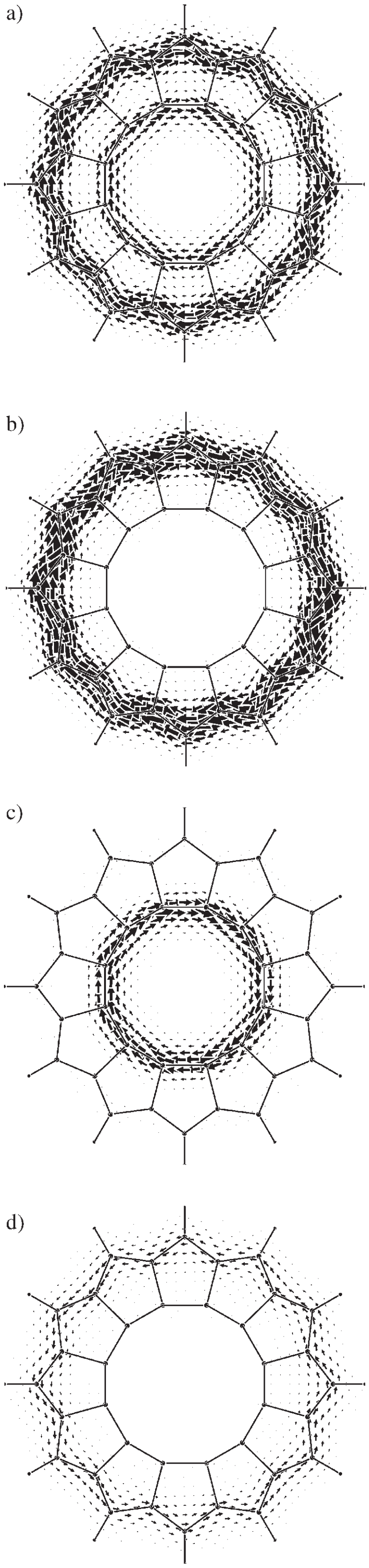

Figure 2. Maps of current density induced in the π system of the [12,5]coronene by a perpendicular external magnetic field on a surface with the molecular shape at $1a_0$ below the saddle. a) Total current density arising from the set of 18 π orbitals and contributions of b) A π HOMO, c) B π HOMO−1, and d) B π HOMO−2 near-degenerate pair. See legend to Figure 1 for computational and plotting details.

unusual magnetism. The calculated currents are strong: the maximum currents in the total-π maps (Figures 1a, 2a) are respectively three and two times the strength of the (diatropic) benzene π ring current calculated by the same approach. Qualitatively, the influence of the above paratropic currents on the molecular properties is expected to be smaller in [8,5]coronene: **2** sustains a ring current that has similar intensity to that in **3**, but it runs around a smaller circuit, and is strong only on one side of the molecular surface.

All the main features of the current maps follow from considerations of pictorial molecular orbital theory. An advantage of the ipsocentric approach is that the sense and strength of current in delocalized systems can be predicted from symmetry and nodal properties of frontier orbitals, and hence can often be rationalized by using approximate π orbitals.[4] Currents arise from virtual excitations from occupied to empty orbitals: paratropic currents from node-preserving, angular-momentum conserving ($\Delta\Lambda = 0$) excitations, and diatropic currents from node-increasing, angular-momentum changing ($\Delta\Lambda = +1$) excitations. In planar $4n$ cycles, the characteristic paratropic current arises from HOMO–LUMO excitation between the Jahn–Teller-split components of an angular-momentum pair. An inevitable companion feature is a weaker diatropic contribution from the HOMO$-$1 to LUMO, corresponding to unit increase in angular momentum on excitation to the LUMO. These contributions have their exact analogues in the present decoupled-circulene systems.

In Hückel (and RHF) pictures, the frontier orbitals of [$4n$,5]coronene are ultimately derived from two pairs of nonbonding orbitals on the separated $4n$ and $8n$ cycles, functions with $\Lambda = n$ and $\Lambda = 2n$, respectively. One $\Lambda = 2n$ function matches the completely antibonding function of the inner cycle; the other $\Lambda = 2n$ function is unmatched and perforce localized on the outer cycle. On introduction of the radial bonds, the Hückel [$4n$,5]coronene retains an accidentally degenerate set of three nonbonding orbitals: two $\Lambda = n$ functions with a radial node, concentrated on the inner cycle, and one function with $\Lambda = 2n$ on the perimeter. The highest formally bonding π orbital (occupied) has $\Lambda = 2n$ and is an in-phase combination of the second perimeter nonbonding orbital with the sole central orbital with the same Λ.

On Jahn–Teller distortion, one member of the $\Lambda = n$ pair is doubly occupied, and this leaves its partner and the perimeter-localized $\Lambda = 2n$ orbital empty. Thus, there are two matched pairs of rotational partners amongst the frontier orbitals of the [$4n$,5] system (Figure 3). Virtual excitation of occupied $\Lambda = n$ (and $\Lambda = 2n$) orbitals accounts for the paratropic circulation on inner (and outer) cycles, in a qualitative $2 \times 2\pi$ description of currents that survives at the ab initio level. Diatropic excitations from the orbitals immediately below are similarly explained.

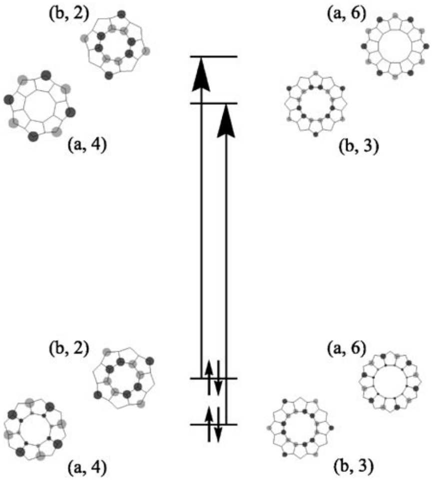

Figure 3. Virtual excitations between frontier orbitals that produce the paratropic ring currents in [8,5]- and [12,5]coronenes. Each orbital is labeled (Γ, Λ) with symmetry Γ (a or b) and angular momentum Λ. In each case, there is a rotationally allowed [(Γ,Λ)$\rightarrow$(Γ,Λ)] excitation from HOMO$-$1 to LUMO and from HOMO to LUMO$+$1. The distribution of coefficients shows that the inner current arises from the HOMO in [8,5]- but HOMO$-$1 in [12,5]coronene, and vice versa for the outer current.

Tables 1 and 2 report second-order magnetic properties of **2** and **3**, respectively, calculated at CTOCD-PZ2[11] and B3LYP/GIAO levels with SYSMO[10] and Gaussian 03[8]

Table 1: Calculated magnetic properties of C_4 [8,5]coronene.[a]

Prop.	CTOCD-PZ2			B3LYP/GIAO		
	$^1/_2(xx+yy)$	zz	Av	$^1/_2(xx+yy)$	zz	Av
σ^{13}C(a)	21(10)	150(6)	64(5)	40(5)	154(7)	78(1)
σ^{13}C(b)	12(2)	26(1)	17(1)	24(2)	44.1(1)	31(1)
σ^{13}C(c)	59(26)	74(9)	64(20)	71(13)	73(8)	71(11)
σ^{1}H(d)	26.5(9)	26.1(2)	26.3(7)	26.5(4)	32.3(5)	28.4(4)
χ	-1856	2772	-314	-2058	13224	3036

[a] Absolute nuclear shielding tensor components are reported in parts per million as averages over inner (a), non-hydrogenated outer (b), and hydrogenated outer sets of carbon centers (c), and hydrogen centers (d). Magnetizability is in 10^{-30} J T^{-2}. The molecule is oriented with z along the main symmetry axis. Figures in parentheses give the variation within the set of atoms. HOMO$-$1$\rightarrow$LUMO and HOMO$\rightarrow$LUMO$+$1 gaps are 0.248 and 0.246 a.u. (HF), 0.067 and 0.060 a.u. (B3LYP).

Table 2: Calculated magnetic properties of C_2 [12,5]coronene.[a]

Prop.	CTOCD-PZ2			B3LYP/GIAO		
	$^1/_2(xx+yy)$	zz	Av	$^1/_2(xx+yy)$	zz	Av
σ^{13}C(a)	10.1(6)	76(2)	32.2(4)	30.3(4)	$-566(1)$	$-169(1)$
σ^{13}C(b)	$-62(2)$	62.5(9)	$-21(1)$	$-24(1)$	$-291(3)$	$-113(1)$
σ^{13}C(c)	46(22)	168(4)	87(16)	54(8)	145(5)	84(10)
σ^{1}H(d)	26.5(6)	40.1(2)	31.0(5)	27.1(3)	242(1)	98.8(3)
χ	-1893	15883	4032	-2631	266835	87191

[a] See footnote to Table 1. HOMO$-$1$\rightarrow$LUMO and HOMO$\rightarrow$LUMO$+$1 gaps are 0.224 and 0.181 a.u. (HF), 0.045 and 0.040 a.u. (B3LYP).

packages, the 6-31G** basis set, and B3LYP/6-31G* geometries (other results for the HF/GIAO can be found in the Supporting Information). At the HF level of theory, which usually underestimates paramagnetism, [8,5]coronene is predicted to show a net out-of-plane paramagnetic component, and, remarkably, [12,5]coronene is expected to be fully paramagnetic. The observed deviation between CTOCD-PZ2 and B3LYP magnetic properties, particularly evident for the out-of-plane components of **3**, can be qualitatively understood in terms of differences between HOMO–LUMO energy gaps (see table footnotes). The B3LYP energy gap is small for both molecules, and this is associated with the tendency of many DFT functionals to exaggerate paramagnetism.[12] On the other hand, the HF predictions have the opposite tendency, that is, transition energies are often overestimated, which leads to exaggeration of diamagnetism. Together, these observations provide strong computational support for the conclusion that **3**, in particular, is overall paramagnetic.

In conclusion, annular molecules comprising 4*n* pentagons have decoupled inner and outer rings which, on both qualitative and quantitative theoretical grounds, are expected to sustain conrotating paratropic ring currents; these currents are strong enough to give a net paramagnetic molecular response, which is rare for closed-shell molecules. We have shown that molecular structures that match desired current patterns can be designed, if not yet synthesized.

Received: October 17, 2006

Keywords: ab initio calculations · annulenes · coronenes · magnetic properties · ring currents

---

[1] a) E. Steiner, P. W. Fowler, L. W. Jenneskens, *Angew. Chem.* **2001**, *113*, 375–379; *Angew. Chem. Int. Ed.* **2001**, *40*, 362–366; b) E. Steiner, P. W. Fowler, L. W. Jenneskens, A. Acocella, *Chem. Commun.* **2001**, 659–660; c) A. Acocella, R. W. A. Havenith, E. Steiner, P. W. Fowler, L. W. Jenneskens, *Chem. Phys. Lett.* **2002**, *363*, 64–72.

[2] J. S. Siegel, T. J. Seiders, *Chem. Br.* **1995**, *31*, 313; J. Aihara, *J. Am. Chem. Soc.* **1992**, *114*, 865–868.

[3] G. Monaco, R. G. Viglione, R. Zanasi, P. W. Fowler, *J. Phys. Chem. A* **2006**, *110*, 7447–7452.

[4] E. Steiner, P. W. Fowler, *J. Phys. Chem. A* **2001**, *105*, 9553–9562; E. Steiner, P. W. Fowler, *Chem. Commun.* **2001**, 2220–2221.

[5] C. D. Stevenson, T. L. Kurth, *J. Am. Chem. Soc.* **1999**, *121*, 1623–1624.

[6] I. Aprahamian, G. J. Bodwell, J. J. Fleming, G. P. Manning, M. R. Mannion, T. Sheradsky, R. J. Vermeij, M. Rabinovitz, *J. Am. Chem. Soc.* **2003**, *125*, 1720–1721.

[7] G. Ege, H. Vogler, *Theor. Chim. Acta* **1972**, *26*, 55–65.

[8] Gaussian 03, Revision B.05, M. J. Frisch et al., Gaussian, Inc., Wallingford, CT, **2004**.

[9] T. A. Keith, R. F. W. Bader, *Chem. Phys. Lett.* **1993**, *210*, 223–231; P. Lazzeretti, M. Malagoli, R. Zanasi, *Chem. Phys. Lett.* **1994**, *220*, 299–304.

[10] P. Lazzeretti, M. Malagoli, R. Zanasi, SYSMO Package, revision 2006, Universities of Modena and Salerno.

[11] a) R. Zanasi, *J. Chem. Phys.* **1996**, *105*, 1460–1469; b) P. Lazzeretti, R. Zanasi, *Int. J. Quantum Chem.* **1996**, *60*, 249–259.

[12] See, for example, S. Patchkovskii, J. Autschbach, T. Ziegler, *J. Chem. Phys.* **2001**, *115*, 26–42, and references therein.